International Journal of Occupational Safety and Ergonomics

Publication details, including instructions for authors and subscription information:
http://www.tandfonline.com/loi/tose20

Deposition and Retention of Ultrafine Aerosol Particles in the Human Respiratory System. Normal and Pathological Cases

Leon Gradoń[a], Dariusz Orlicki[a] & Albert Podgórski[a]

[a] Department of Chemical and Process Engineering, Warsaw University of Technology, Poland

Published online: 08 Jan 2015.

To cite this article: Leon Gradoń, Dariusz Orlicki & Albert Podgórski (2000) Deposition and Retention of Ultrafine Aerosol Particles in the Human Respiratory System. Normal and Pathological Cases, International Journal of Occupational Safety and Ergonomics, 6:2, 189-207

To link to this article: http://dx.doi.org/10.1080/10803548.2000.11076451

INTERNATIONAL JOURNAL OF
OCCUPATIONAL SAFETY AND ERGONOMICS 2000, VOL. 6, NO. 2, 189–207

Deposition and Retention of Ultrafine Aerosol Particles in the Human Respiratory System. Normal and Pathological Cases

Leon Gradoń
Dariusz Orlicki
Albert Podgórski

Department of Chemical and Process Engineering,
Warsaw University of Technology, Poland

The particle number concentration in ambient air is dominated by nanometer-sized particles. Recent epidemiological studies report an association between the presence of nanoparticles in inhaled air at the workplace and acute morbidity and even mortality in the elderly. A theoretical model of deposition of 20 nm particles in the human alveolus was formulated. Gas flow structure and deposition rate were calculated for alveoli with different elastic properties of lung tissue. Data obtained in the paper show increased convective effects and diffusional rate of deposition of nanoparticles for alveoli with higher stiffness of the alveolar wall. The retention of deposited particles is also higher in these pathological alveoli. Results of our calculations indicate a possibility of existence of a positive loop of coupling in deposition and retention of nanoparticles in the lung with pathological changes.

nanoparticles clearance deposition retention toxicity

1. INTRODUCTION

Solid and liquid aerosols in the atmosphere originate from both natural and industrial sources. Inhalation of those aerosols from ambient air results in

This work is part of the National Strategic Programme "Occupational Safety and Health Protection of Man in the Working Environment," supported in 1998–2001 by the State Committee for Scientific Research of Poland. The Central Institute for Labour Protection is the Programme's main co-ordinator.

Correspondence and requests for reprints should be sent to Leon Gradoń, Department of Chemical and Process Engineering, Warsaw University of Technology, ul. Waryńskiego 1, 00-645 Warszawa, Poland. E-mail: <gradon@ichip.pw.edu.pl>.

the introduction and deposition of various particulate substances in the human respiratory tract, creating a potential health hazard. The assessment of this hazard and appropriate countermeasures to be taken require understanding and estimating local and regional deposition of inhaled particles in the respiratory tract. Assessment of the toxicity of airborne pollutants can be accomplished through epidemiological studies of morbidity and mortality patterns in humans. Pollutant toxicity is also determined by studies in which animal subjects are exposed to a toxic aerosol in order to predict possible toxic effects on human. It appears from experimental data that under high exposure condition (mg/m^3 range) of large-sized particles ($d > 0.2$ μm), it will induce toxic effects. These effects include pulmonary fibrosis and lung tumours, which are associated with a phenomenon of lung particle overload. It was observed (Oberdörster, Gelien, Ferin, & Weiss, 1995) that freshly generated ultrafine particles, when inhaled as singles at very low mass concentration (order of $\mu g/cm^3$), can be highly toxic to the lung. Ultrafine particles have high deposition rate efficiency in the lower respiratory tract, large numbers per unit mass, and increased surface areas available for interaction with cells. In addition, particles-cells interactions could be potentially amplified by the presence of radicals on these surfaces. Ultrafine particles when deposited on the surface of alveolar epithelium penetrate rapidly into the pulmonary interstitium. With long-term exposure of ultrafine particles, lung clearance processes are overwhelmed, inflammation persists, and lung burden increases. This causes the pathogenesis of the lung structure (fibrosis; McClellan, 1996). The aforementioned effects indicate that ultrafine particles like carbon black, combustion nuclei, oil smokes, metallurgical dusts, and fumes frequently present at the workplace can be highly toxic and it is necessary to study their balance when inhaled. The aim of this study is to model deposition and retention of ultrafine particles for healthy and pathologically changed lungs. Fibrosis as an effect of lung exposure to ultrafine particles is considered. We would like to see if pathologically changed lungs create a positive loop of coupling in lung damage.

2. PARTICLE RETENTION IN LUNGS

The time dependent mass of particulate in the pulmonary region of human lungs is described in the present model. An accurate quantitative description of aerosol retention requires a clearly defined region of observation, such as

a part of the respiratory system or a differential element in the generation of the bronchial tree, alveoli, or nasopharynx. It is assumed, particularly, that material deposited in the nasopharynx is removed much more rapidly than the particulate in the remaining regions of the respiratory system, and these play no role in the retention phenomena (Dahlback, Eirefelt, Karberg, & Nebrink, 1989). In the differential equations on which this model is based, the smallest region for the mass balance of the particulate matter is a single generation in the dichotomy model of the lungs. Therefore, the mass balance equation for particle retention in an i-th generation is

$$\frac{dm_i}{dt} = Q_{i+1} - Q_i + R_i - (A_i)_{pulm} \tag{1}$$

where m_i denotes the mass of material contained in the i-th generation, Q_{i+1} is mass flow rate into the i-th generation from the $i + 1$ generation through mucociliary action, Q_i is the mass flow rate leaving the i-th generation, R_i is the mass deposition in the i-th generation originating from the particulate rich air flowing through that generation, and $(A_i)_{pulm}$ is the rate of particle transport through pulmonary clearance and particulate translocation to the pulmonary parenchyma. In addition to that generalised mass balance, a complete mathematical model of particle retention in the human lungs includes the morphology and geometry of a respiratory system.

3. RATE OF PARTICLE DEPOSITION IN A RESPIRATORY SYSTEM

The simplest and most widely used geometrical configuration for the lungs is the symmetrical lung model proposed by Weibel (1963). The bronchial tree is assumed to consist of an expandable pulmonary region where a respiratory gas exchange takes place and a bifurcating series of parallel and semirigid cylindrical tubes of the tracheobronchial tree. The geometry of a bifurcation is described by three classes of second order functions (Gradoń & Orlicki, 1990). The air velocity profile within each bifurcation is found from the solution of the quasi steady-state Navier-Stokes equation. The average velocity at the entrance to any generation is estimated from the volumetric flow rate, which in turn is governed by both the lung tidal volume TV and breathing frequency f_b. The gas flow structure and the mass of particles suspended in it determine the deposition rates of particles. For

ultrafine particles considered in this paper the main mechanism of deposition under flow conditions in the respiratory tract is convective diffusion.

The contribution of convection and diffusion can be estimated through their characteristic times. The characteristic time of convection, t_c, is defined as the time needed for the frontal surface of inspired gases to cross the generation i.

The characteristic time of diffusion, t_d, is defined as the time needed for a volume of gas equal to the duct volume to pass the duct entry by diffusion (Paiva, 1972).

According to that definition, for a person breathing with 750 cm^3 TV and a 4-s symmetric breathing cycle period, the inspired air arrives predominantly by convection up to the 20th generation in the Weibel model of the lung, and attains them by diffusion. A short residence time of the aerosol in the upper generations of the tracheobronchial tree causes that ultrafine particles deposit in that region with very low efficiencies. This was proved, for the purpose of this paper, using the procedure of calculation described by Gradoń and Orlicki (1990).

According to our earlier analysis (Gradoń & Podgórski, 1996b; Napiórkowski, 1980), for particles with high diffusivity, the main region at their deposition are generations 21–23 for which an alveolus is the main component of a structure.

4. ULTRAFINE PARTICLE DEPOSITION IN A SINGLE ALVEOLUS

There are many approaches to calculating the deposition of aerosol particles in the pulmonary region of human lungs. For ultrafine particles, local gas velocity and particle diffusion are the main parameters that define deposition rate. Macro-transport particles models (Edwards, 1995) or Monte Carlo simulations are used for analysing the deposition rate for assumed geometry and flow conditions. To emphasise the effect of lung diseases, which affects the local flow structure, properties of lung elasticity should be incorporated into the model. According to Kaminsky and Irvin (1997), that parameter controls gas flow rate for a given transmembrane pressure difference. Taking into account all limitations, mass balance with incorporation of wall deformation based on the elastic stress approach is used for modelling diffusional particles in the human lung.

Lungs lie within the chest cavity in which ribs form the sides and the diaphragm forms the floor. When chest dimensions change due to the action

of different muscles, lung volume is modified virtually to the same degree because of the change in intrapleular pressure. A model to simulate ventilation and particle deposition consists of a tube (respiratory bronchiole) closed at the end with an elastic spherical balloon (an alveolus) with the other end connected with surroundings through extra resistance to gas flow. It represents resistance to air flow through nose, pharynx, larynx, trachea, and all generations of airways preceding respiratory bronchioles. This structure is placed inside a cylinder in such a way that the tubular part protrudes through the cylinder wall and opens to the environment (Figure 1a). The cylinder (the thorax) is closed with a moving piston (the diaphragm, which regulates inside—intrapleural—pressure). When the piston is pulled out by an external force, the pressure inside the cylinder decreases, the elastic walls of the balloon stretch, the pressure inside the balloon drops below atmospheric pressure, and air is drawn through the extra resistance. This sequence of events corresponds to the inspiration part of the breathing cycle. When the external force is relaxed, the piston moves until the pressure inside and outside equalises. The elastic walls of the balloon recoil and the air flows outside. This sequence of events represents the expiration part of the breathing cycle. The air flow inside an alveolus is a result of pressure difference $\Delta p = Po - P(t)$, and the mechanistic properties of the

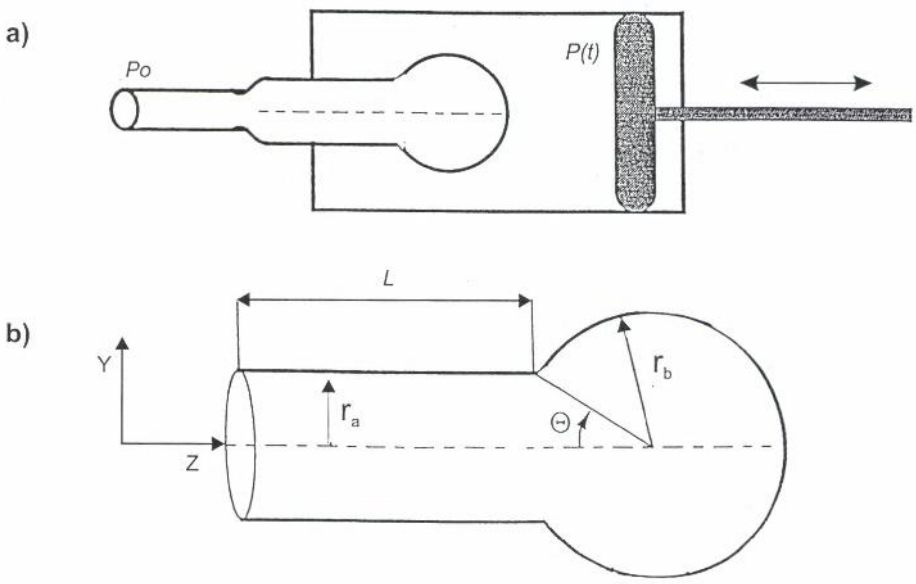

Figure 1. Model of (a) lung ventilation, (b) geometrical configuration of the alveolus.

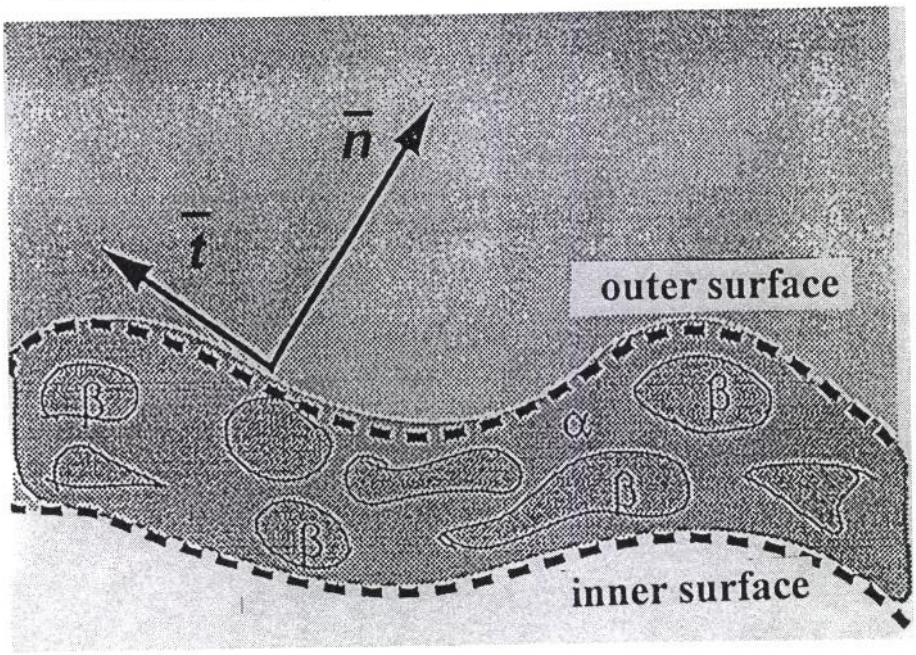

Figure 2. Two-phase continuum model of lung wall tissue.

alveolar wall. Alveoli walls contain a dense network of capillaries and reticular, collagenous, and elastic fibres. The non-linear response of alveolar wall tissue can be represented by a two-phase continuum model based on the theory of mixtures (Simon, Kaufmann, McAfee, & Baldwin, 1993). The tissue (Figure 2) consists of an incompressible, elastic porous solid skeleton (β-phase) saturated with viscous fluid (α-phase). A model describing the dynamics behaviour of an alveolus during the breathing cycle includes conservation equations for mass and momentum conservation and kinematic equations for wall deformation. The model is additionally supplied with air flow and aerosol transport equations.

Wall deformation model

A local normal force balance between viscous and elastic stress, surface tension, and gas pressure is used to evaluate wall deformation of an alveolus, whose geometry is shown in Figure 1a.

Continuity equation

$$\nabla(\varphi_\alpha \mathbf{w}_\alpha + \varphi_\beta \mathbf{w}_\beta) = 0 \tag{2}$$

where ∇—nabla operator, φ—volume fraction, $\mathbf{w}$—velocity of the phase.

Momentum equation

$$\rho_\alpha \frac{D\mathbf{w}_\alpha}{Dt} + \nabla\overline{\sigma}_\alpha - \pi_\alpha = 0, \text{ for } \alpha\text{-phase} \tag{3}$$

$$\nabla\overline{\sigma}_\beta + \pi_\beta = 0, \text{ for } \beta\text{-phase} \tag{4}$$

where ρ_α is the apparent density of α-phase, D/Dt is the substantial derivative, σ is the Cauchy stress tensor, π is the diffusive momentum exchange between the two phases.

Constitutive equation

$$\overline{\sigma}_\alpha = -\varphi_\alpha p\overline{\mathbf{I}} \tag{5}$$

$$\overline{\sigma}_\beta = -\varphi_\beta p\overline{\mathbf{I}} - \lambda_\beta\overline{\mathbf{I}} + 2\mu_\beta\overline{\mathbf{I}} \tag{6}$$

$$\pi_\beta = -\pi_\alpha = \mathbf{k}(\mathbf{w}_\alpha - \mathbf{w}_\beta) \tag{7}$$

where p is apparent pressure, $\mathbf{I}$ is identity tensor, λ is Lamé constant, μ is the modulus of elasticity and $\mathbf{k}$ is drag coefficient.

Boundary conditions

$$\mathbf{n} \cdot \overline{\sigma}|_{r=R_i} = \mathbf{n}p_{il} + \mathbf{n}\chi, \text{ for inner surface} \tag{8}$$

$$\mathbf{n} \cdot \overline{\sigma}|_{r=R_0} = \mathbf{n}p(t), \text{ for outer surface.} \tag{9}$$

Kinematic equation

$$\mathbf{n}\frac{d\mathbf{r}}{dt} = \mathbf{n}\mathbf{w}_\alpha \tag{10}$$

where $\mathbf{n}$ stands for a vector normal to the surface and χ is surface curvature.

Air flow field

The deformation of alveolus walls creates pressure gradients inside the alveolus and then air flow follows. To determine the fluid flow field, the continuity and momentum balance equations for air are solved.

Continuity equation

$$\nabla \mathbf{v} = 0 \tag{11}$$

$$\rho_{air} \frac{D\mathbf{v}}{Dt} = -\nabla \sigma_{air}. \tag{12}$$

Boundary condition

$$\mathbf{v} = \mathbf{w}, \text{ at the inner wall}$$

$$\mathbf{n}\bar{\sigma}_{air} = \mathbf{n}(p_0 - p_{al}), \text{ at alveolus entrance} \tag{13}$$

where $\mathbf{v}$—air velocity, ρ_{air}—air density.

Particle motion and deposition

Concentration c of ultrafine particles in the alveolus is described by the time dependent connective diffusion equation

$$\frac{dc}{dt} + \mathbf{v}\nabla c = D_p \nabla^2 c \tag{14}$$

where D_p—particle diffusivity.

It was assumed that at the alveolar opening concentration is uniform. The rate of particle deposition on the walls is given as

$$j = -\int_{\Omega_0}^{\pi} D_p \left(\frac{\partial c}{\partial t}\right)_{r=r_b} 2\pi r_b^2 \sin\theta d\theta \tag{15}$$

and the accumulated particle loss t_0 to t is then

$$J = \int_{t_0}^{t} j dt. \tag{16}$$

The model just formulated was solved numerically by using the finite element method (Gallagher, Simon, Johnson, & Gross, 1982), where the functional is defined by the Galerkin method. The domain was discretised into isoparametric rectangular elements and Lagrangian polynomials were used as basis functions. For time integration, the explicit Adam-Bashfort

predictor method with an implicit trapezoid corrector was used. As a result of these procedures a set of non-linear equations was obtained and solved by the modified Newton-Raphson interactive method. In order to reduce the computational effort, the physical domain, which undergoes changes of shape, area, and volume, was mapped out of the unchangeable computational domain. Such a procedure makes it possible to model the deformation of bodies with complex geometry. Calculations were done for the following set of parameters defined in the model (Equations 2–16): geometry of alveolus (Figure 1b), $r_a = 2.05 \cdot 10^{-4}$ (m); $L = 2 \cdot 10^{-4}$ (m); $r_b = 2.5 \cdot 10^{-4}$ (m); alveolar wall thickness $\Delta = 1.0 \cdot 10^{-4}$ (m); properties of poroelastic body (Figure 2), Lamé constant $\lambda = 5714$ (N•m); modulus of elasticity $\mu = 1375$ (n•m^{-2}); volume fraction of α-phase $\varphi_\alpha = 90\%$, $\varphi_\beta = 10\%$. The drag coefficient **k** was estimated as equal to 20% of a drag at air flow; density of α-phase $\rho_d = 999.8$ (kg•m^{-3}); and viscosity $\mu = 1.8 \cdot 10^{-3}$ (Pa•s). Air flow calculations were made for a respiratory cycle of $7.5 \cdot 10^{-4}$ (m^3) tidal volume and a 4-s period of breathing. It was assumed that inspiration and expiration have equal duration in the cycle and there is no pause between the parts. Air density was assumed to be equal to $\rho_{air} = 1.29$ (kg•m^{-3}), and viscosity $\mu_{air} = 1.71 \cdot 10^{-5}$ (Pa•s). The transmembrane pressure difference was 1960 (N•m^{-2}). For calculating aerosol particle deposition, submicron particles of 20 nm were used, their diffusion coefficient was $D_p = 1.34 \cdot 10^{-8}$ (m^2•s^{-1}).

5. RESULTS OF CALCULATIONS

The deposition process of particles for which the predominant mechanism of transport is connective diffusion occurs close to the wall, where particles are collected. In the analysis of connective diffusion problems (Equation 15), it is important to estimate a relation between the thickness at momentum and mass transfer boundary layers. These thicknesses are a result of simultaneous diffusion and flow of particles. Information on the convective diffusion effect is included in the value of the connective mass transfer coefficient k_c. Particles flux lost from the surrounding fluid at the surface of a vessel is proportional to the average particle concentration in a gas with coefficient of proportionality k_c. A concept often useful in modelling a mass transfer process follows from the assumption that it occurs in the slow-moving gas layer adjacent to the surface of the vessel-boundary layer. If the "stagnant" film thickness δ is chosen so that the fluid film alters the same resistance to

diffusion as encountered in the combined process of molecular diffusion and diffusion by mixing of the moving fluid, $k_c = D/\delta$. The local motion of the fluid strongly affects the deposition. The numerical solution of the problem (Equations 2–14) with parameter data indicated in the set of parameters of the model shows that the relative velocity of the air near an alveolar wall is very low. For a perfectly elastic wall (for assumed values model parameters), inertia of inhaled air and inertia of the wall are similar. Air follows the alveolar wall displacement. The pathological case assumed here is related to lung fibrosis. In a normal individual lung elastic recoil increases with increasing lung volume in a non-linear fashion. In the case of increased lung elastic recoil (fibrosis) the relation between the volume of inhaled air and transpulmonary pressure indicates a significant increase of the difference of the gas and tissue inertia (Kaminsky & Irvin, 1997). To see this effect we have calculated the model (Equations 2–14) for increased Young's modulus of elasticity of the alveolar tissue 30% compared to the perfectly elastic tissue. The result of calculations of the local gas velocity in the alveolus is shown in Figure 3. Figure 3a indicates velocities at the beginning of inspiration, Figure 3b at the end of inspiration, whereas 3c shows velocity of particles at the beginning of expiration, and 3d at the end of expiration. The length of the arrow is proportional to gas velocity and the arrow indicates the direction of the flow. Generally gas flow occurs mostly in the centre of the alveolus. Local velocities of the gas at the wall increase for the transition between inspiration and expiration. The relative velocity of a gas and wall is higher for increased lung elastic recoil (fibrosis). It is in very good agreement with the observation of the so-called "fast" and "slow" alveolus behaviour (Nunn, 1977). According to the aforementioned aspects, it can increase the diffusional deposition of ultrafine particles in the alveolus. In the next step of our analysis, the rate of fractional deposition (j/M) of particles as a function of time during a cycle for the steady-state condition was calculated (Equations 15–16). The steady-state deposition was reached in the 5th cycle of breathing. The total number of particles M entering into the alveolus in a respiratory cycle was calculated from the balance of particles for the assumed average number concentration of particles at the entrance to the cylinder attached to the alveolus, duration time, and flow conditions. The results are shown in Figure 4. One can see that the convective effect discussed here, which is the result of increased stiffness of the alveolar wall fibrosis, increases the rate of deposition of ultrafine particles. It is also observed that the rate of fractional deposition

increases significantly at the moment of transition between inspiration and expiration.

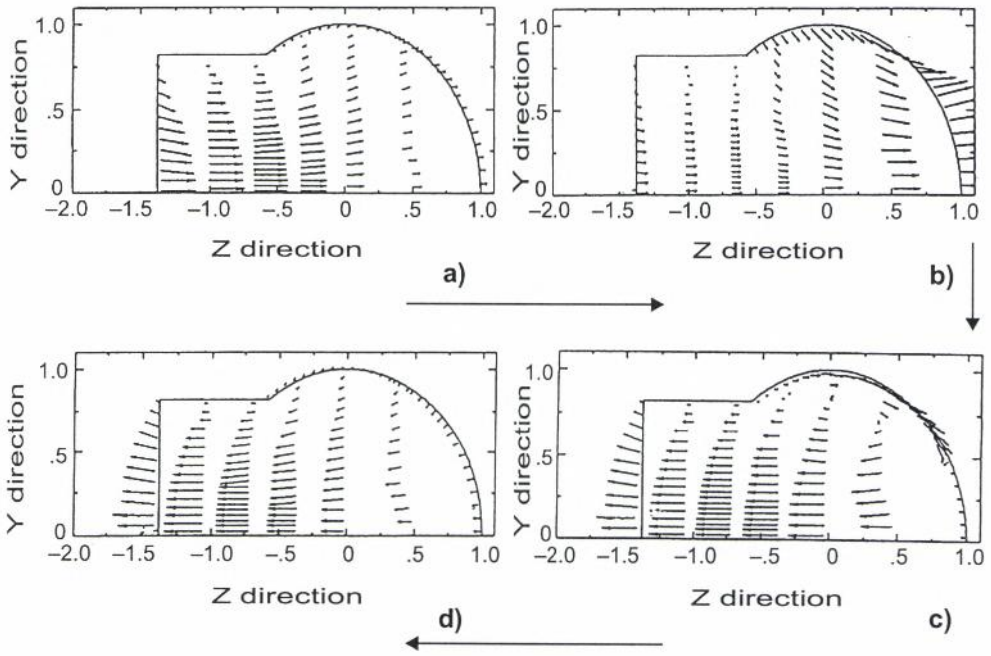

Figure 3. Flow structure of air in the alveolus during (a, b) inspiration and (c, d) expiration.

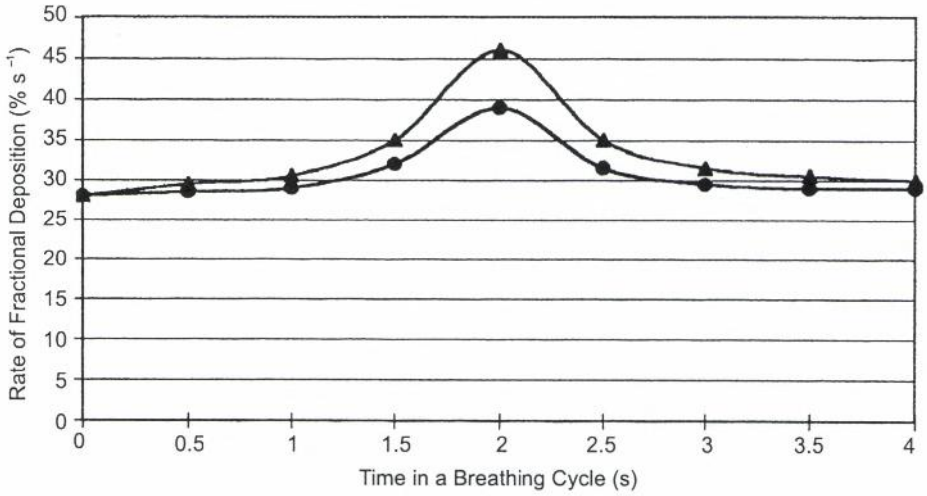

Figure 4. Rate of fractional deposition of 20 nm particles in the alveolus during steady-state breathing.

6. RETENTION OF INHALED PARTICLES

Clearance mechanisms

The ultrafine particles considered in this paper are assumed to be insoluble. When deposited in the lungs, they are gradually eliminated by means of several mechanisms. In tracheobronchial or conducting airways, mucociliary clearance is the most important mechanism. Particles deposited on the surface of mucus are transported into the pharyngeal region as the mucus is propelled by the rhythmic beating of cilia. Taking into account rheological properties of mucus (Gilboa & Silberberg, 1976) and cilia beating pattern (Sleigh, 1981), the rate of mucociliary clearance was calculated (Gradoń & Yu, 1986).

In our case, when ultrafine particles, which are mostly deposited in the respiratory zone, are considered the mucociliary escalator serves as a transporter of deposits coming from the pulmonary region.

Particles deposited in the pulmonary region of the respiratory system (generation 17–23) exist as "free" and phagocytosed by alveolar macrophage (AM) particles at any given instant. Both forms of deposits are withdrawn by a mucociliary escalator and subsequently propelled into the lung's interstitial, lymph nodes, and finally into the blood system.

The estimation of residence time for both forms of particles in the pulmonary region of the lung is uncertain. Recent publications on lung clearance include relatively insufficient information on macrophage mobility and its translocation velocity from the alveoli to the mucociliary escalator. Morrow (1989) suggests two general mechanisms of AM translocation. The first is that of directed migration through airways to the mucociliary escalator. In this case, AM migration is presumed to be due to either directed motion of the alveolar lining layer on which the AM are placed, as well as free deposited particles are passively transported by hydrodynamic effects caused by the surface tension gradient in the surfactant monolayer adsorbed on the hypophase (Podgórski & Gradoń, 1991, 1993).

Motion may also arise from the chemoattractant gradient, which directly polarises and facilitates AM migration on the alveolar epithelial surface. Macklin (1955) proposed another concept of directional movement based on the assumption of the continuous capillary effusion into the alveoli, but this theory is still not elaborated in detail. The second mechanism for the translocation of the macrophages assumes the motion not to be directional, but a random walk as a result of chemotactic displacement of AMs (Gradoń & Podgórski, 1995). The average residence time for balanced deposits in the pulmonary region of lungs τ_a is given as

$$\tau_a = \phi \cdot \tau_d + (1 - \phi) \cdot \tau_{ch} \tag{17}$$

where ϕ is the mass fraction of the deposits that exist as free particles, τ_d is the average particle residence time of AMs loaded with particles.

There is a second proposed pathway for deposits to enter the pulmonary region. It is the slow phase of displacement of the particles into the lung parenchyma, followed by entrance into the blood system.

In the model (Gradoń & Podgórski, 1991), we assume that this slow phase is composed of two stages. In the first stage, part of the deposited material contained in the alveoli and terminal bronchiale of a given generation is transferred to the wall of the lung tissue at a constant rate K. The material is then transported to the lymphatic and blood system at a rate Λ. The value of the transfer constant K is determined by the permeability of the lung parenchyma membrane subjected to free and phagocytosed particles. The value of the coefficient Λ is a function of cell metabolism.

Retention curve

Figure 5 shows control areas for mass balance of the particulate matter retained in the airways of the respiratory system. In accordance with the Weibel schematic presentation (Weibel, 1963), the lung has been divided into a conducting part consisting of generations 0–16, and a respiratory part with generations 17–23. Because of the physical properties of the surfaces in the respiratory region and the long residence times there, a fraction of the deposited matter is transported from the air space to the lymphatic and blood systems, an effect that can be neglected in the conductive section. The kinetic equation of retention (Gradoń & Podgórski, 1991) describes time variation of the mass in the region under consideration. The amount of deposited particles is expressed in the form of surface concentration C_i (number of particles per unit surface of the airways S_i of the respiratory system) at a given i-th generation. In the balance equation for a selected generation, i, an average flux R_i of the particles deposited in the generation, a flux of particles transferred from the generation $i + 1$ in a clearing transport, and a flux of particles leaving the generation i contribute to the time variation of C_i. Transport rate into the lung parenchyma and blood characterised by coefficients K and Λ contributes to the balance in the pulmonary region.

Retention of particles, $R(t)$, determined as the amount of particles retained at a given moment in the respiratory system was calculated from the mathematical model described in detail in the paper by Gradoń and Podgórski (1991).

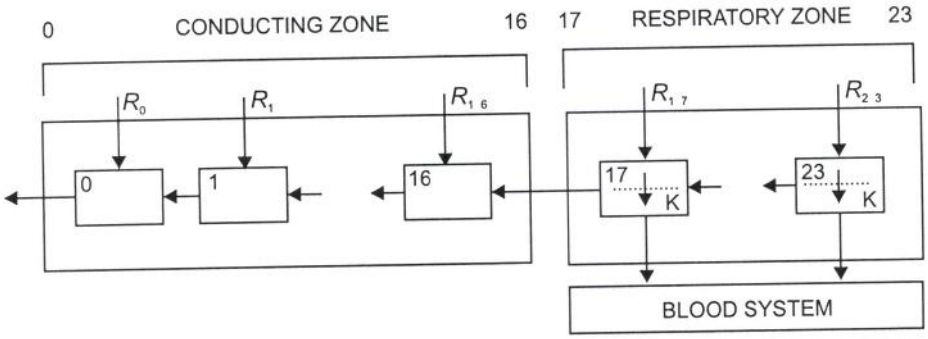

Figure 5. Schematic representation of the retention model based on Weibel's model of the lung.

For the conductive section (Figure 5), the equation for mass balance takes the form

$$\frac{dC_i^a}{dt} = R_i + \frac{S_{i+1}}{S_i} \cdot \frac{C_{i+1}^a}{\tau_{i+1}} - \frac{C_i^a}{\tau_i} \qquad 0 \le i \le 16. \tag{18}$$

Equations for the pulmonary section have the form

$$\frac{dC_i^b}{dt} = R_i + \frac{S_{i+1}}{S_i} \cdot \frac{C_{i+1}^b}{\tau_{i+1}} - \mathrm{K} \cdot C_i^b \qquad 17 \le i \le 23 \tag{19}$$

$$\frac{dC_i^c}{dt} = \mathrm{K} \cdot C_i^b - \Lambda \cdot C_i^c. \tag{20}$$

Retention of particles, $R(t)$, is calculated from

$$R(t) = \sum_{i=0}^{23} [C_i^a(t) + C_i^b(t) + C_i^c(t)] \cdot S_i. \tag{21}$$

The system of equations (18–21) is completed with the initial condition $C_i^{abc}(0) = 0$ and the continuity condition $C_{16}^a = C_{16}^b$.

Relative retention $R(t)$ related to deposited particles as a function of post-exposure time for the inhalation of 20 nm particles was calculated. Fluxes R_i at alveolated generations were computed from the aforementioned model assuming tidal volume 750 ml and a symmetrical 4-s breathing cycle. Particle mass concentration in inhaled air was equal to 10^5 particles/cm^3 and exposure time was 8 hrs.

Residence times and deposition rates at a particular generation for a normal lung are collected in Table 1.

TABLE 1. Total Areas, S_i, Mean Residence Times, τ_i, and Deposition Fluxes, r_i, for Generations of the Human Respiratory System. Particles 20.0 nm in Diameter

Generation	0	1	2	3	4	5	6	7	8	9	10	11	12
$S_i \cdot 10^{-3}$ mm^2	6.786	3.649	1.982	1.070	2.873	3.765	5.067	7.092	9.574	13.380	19.240	27.350	40.340
τ, min	4.90	4.54	2.33	1.11	3.31	3.70	4.66	6.03	7.44	9.64	12.70	16.30	22.00
$R_i \cdot 10^{-3}$ m$^{-2}\cdot$s^{-1}	—	—	—	—	—	—	—	—	—	—	—	—	—

Generation	13	14	15	16	17	18	19	20	21	22	23
$S_i \cdot 10^{-3}$ mm^2	56.98	87.61	135.9	203.80	442.20	893.60	1900.00	4118.00	8236.00	16470.00	2800.00
τ, min	27.00	38.30	50.00	55.00	100.00	250.00	530.00	790.00	930.00	1180.00	1500.00
$R_i \cdot 10^{-3}$ m$^{-2}\cdot$s^{-1}	—	—	—	—	—	—	65	51	48	48	40

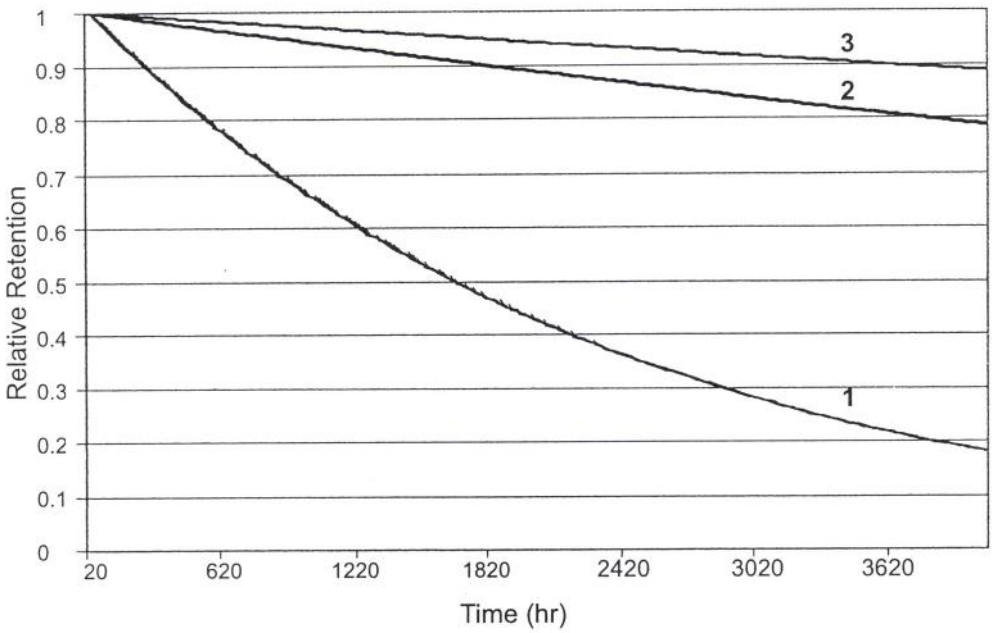

Figure 6. Relative retention curves for a normal curve (1) and pathological cases (curves 2 and 3).

The results of calculating the relative retention curve are shown in Figure 6. Curve 1 represents dynamics of retention for the model of a normal alveolus. Particles 20 nm in diameter, according to the analysis presented in this paper, deposit in the pulmonary region of the respiratory system. The retention curve does not include the fast clearance stage, because there are no deposited particles in the tracheobronchial tree where fast mucociliary clearance operates. Particles presented in the pulmonary region are removed by directional displacement due to the activity of the surfactant, due to phagocytosis, and finally they are translocated into lung parenchyma. The half-time of clearance, defined as time in which 50% of deposits are removed out of the lung, equals 51 days.

For pathological alveoli (fibrosis), deposition rates R_i for the same condition of inhalation were approximately 20% higher than for normal alveoli. Residence times τ_i in pathological alveoli due to a reduction of surfactant activity and overloading of macrophages (Gradoń & Podgórski, 1996a) were about 5 times longer than for normal alveoli (Table 1).

The calculated retention curve for that case, even for significantly slower clearance rate in the air space of alveolus, gives almost the same curve as curve 1. Both curves overlap in Figure 5. Calculated $\tau_{1/2}$ for that

case was only a few percent longer than for a normal alveolus. An increased retention of particles in the lungs with fibrosis observed in experiments is caused probably by a changed structure of the lymphoid layer of lung parenchyma. The releasing of included particles in that region into the blood system is slower than for normal lungs (Foster, Pearman, & Ramsden, 1989). In relation to the model just formulated it means a decrease of the value of parameter Λ. To simulate the influence of that effect on retention, we calculated the relative retention for pathological lung, assuming $\Lambda = 1 \cdot 10^{-6}$ min^{-1} (curve 2 in Figure 5) and $\Lambda = 5 \cdot 10^{-7}$ min^{-1} (curve 3 in Figure 5). Calculated $\tau_{1/2}$ for curve 2 was equal to 485 days and for curve 3 it was equal to 950 days.

The results of calculation indicate a very strong influence of the metabolism of the transformation of deposits and their releasing from lung parenchyma into the blood on the retention of particles in the lungs. This effect is particularly strong for the stiffer structure of lungs. Increased deposition rate and slower clearance for the lung with fibrosis can create a synergetic toxic effect for such pathology when exposed to a high concentration of nanoparticles.

7. CONCLUSION

The mathematical model of particle deposition and retention in the lung presented in this paper gives the possibility of an analysis of the influence of lung pathology on the behaviour of inhaled particles. The results of calculations indicate the specific flow structure in an alveolus with stiffer tissue. The strong convective effect, especially at the transition between inspiration and expiration, causes an increase of the deposition rate of nanoparticles in the alveolus. The increased deposition rate and the overloading of the pathological alveoli with deposits prolong a clearance effect in the pathological alveolus.

If, in addition, the rate of releasing of deposits from lung parenchyma into the blood system is slow, it can create significant structural changes in lung parenchyma.

SYMBOLS

p — pressure, N$\cdot$m^{-2}
$\mathbf{w}$ — vector of the phase velocity, m$\cdot$s^{-1}
$\bar{\mathbf{I}}$ — identity tensor

$\mathbf{n}$ — orientation vector normal to the surface
$\mathbf{v}$ — gas velocity, $m \cdot s^{-1}$
C — particle number concentration, m^{-3}
D_p — particle diffusion coefficient, $m^2 \cdot s^{-1}$
$\mathbf{j}$ — particle flux, $m^{-2} \cdot s^{-1}$
K — constant in the retention model, s^{-1}
S — surface of lung airways, m^2
t — time, s
R — relative retention
R_i — rate of particle deposition in i-th generation
r_a — radius of the alveolus
r_b — radius of bronchioli
φ — volume fraction of the phase
$\overline{\sigma}$ — Cauchy stress tensor, $N \cdot m^{-2}$
π — diffusive momentum exchange, $N \cdot m^{-3}$
Λ — constant in the retention model, s^{-1}

REFERENCES

Dahlback, M., Eirefelt, S., Karberg, I.B., & Nebrink, O. (1989), Total deposition of Evans blue in aerosol exposed rats and guinea pigs. *Journal of Aerosol Science, 20*, 1125–1127.

Edwards, D. (1995), The macrotransport at aerosol particles in the lung: Aerosol deposition phenomena. *Journal of Aerosol Science, 26*, 293–317.

Foster, P.P., Pearman, I., & Ramsden, D. (1989). An interspecies comparison of the lung clearance of inhaled monodisprese particles. *Journal of Aerosol Science, 20*, 189–204.

Gallagher, R.M., Simon, B.R., Johnson, P.C., & Gross, J.F. (1982). *Finite elements in biomechanics*. New York, NY, USA: Wiley.

Gilboa, A., & Silberberg, A. (1976). In situ rheological characterisation of epithelial mucus. *Biorheology, 17*, 163–167.

Gradoń, L., & Orlicki, D. (1990). Deposition of inhaled aerosol particles in a generation of the tracheobronchial tree. *Journal of Aerosol Science, 21*, 3–14.

Gradoń, L., & Podgórski, A. (1991). Kinetics of particle retention in the human respiratory tracts. *Annals of Occupational Hygiene, 35*, 249–262.

Gradoń, L., & Podgórski, A. (1995). Displacement of alveolar macrophages in air space of human lung. *Medical & Biological Engineering & Computing, 33*, 575–581.

Gradoń, L., & Podgórski, A. (1996a), Alveolar macrophage (AM) mobility reduction a result of long-term exposure to high dust concentration in inhaled air. *International Journal of Occupational Safety and Ergonomics, 2*(2), 137–147.

Gradoń, L., & Podgórski, A. (1996b), Deposition of inhaled particles. Discussion of present modelling techniques, *Journal of Aerosol Medicine, 9*, 343–355.

Gradoń, L., & Yu, C.P. (1986). Rate of mucociliary clearance. In J.-M. Aiache (Ed.), *Proceedings of ISAM* (pp. 201–216). Paris, France: Laboratoir Lavoisier.

Kaminsky, D.A, & Irvin, Ch.G. (1997). Lung function in asthma. In P.J. Barns (Ed.) *Asthma* (pp. 1277–1299). New York, NY, USA: Lippincott-Raven.

Macklin, C.C. (1955). Pulmonary sumps, dust accumulation, alveolar fluid and lymph vessels. *Acta Anathomica, 23*, 1–33.

McClellan, R.O. (1996). Lung cancer in rats from prolonged exposure to high concentration of particles: Implication to human risk assessment. *Inhalation Toxicology, 8*, 193–226.

Morrow, P.E. (1989). Possible mechanisms to explain dust overloading of lung. *Fundamental & Applied Toxicology, 10*, 369–378.

Napiórkowski, J. (1980). *Depozycja aerozoli w pęcherzyku płucnym* [Aerosol deposition in pulmonary alveoli]. Unpublished diploma thesis, Politechnika Warszawska, Warsaw, Poland.

Nunn, J.F. (1977). *Applied respiratory physiology*. London, UK: Butterworth.

Oberdörster, G., Gelien, R.M., Ferin, J., & Weiss, B. (1995). Association of particulate air pollution and acute mortality. Involvement of ultrafine particles? *Inhalation Toxicology, 7*, 111–124.

Paiva, M. (1972). Computation of the boundary conditions for diffusion in the human lung. *Computers and Biomedical Research, 5*, 585–595.

Podgórski, A., & Gradoń, L. (1991). Function of the pulmonary surfactant in the clearance of respiratory bronchioles. *Chemical Engineering Communication, 110*, 146–162.

Podgórski, A., & Gradoń, L. (1993). An improved mathematical model of hydrodynamical self-clearance of pulmonary alveoli. *Annals of Occupational Hygiene, 37*, 347–365.

Simon, B.R., Kaufmann, M.V., McAfee, M.A., & Baldwin, A.L. (1993). Finite element models for arterial wall mechanics. *Journal of Biomechanical Engineering, 115*, 489–496.

Sleigh, M.A. (1981). Ciliary function in mucus transport. *Chest, 80*, 791–795.

Weibel, R. (1963). *Morphometry of the human lung*. Berlin, Germany: Springer.